MINIMUM SURFACE-EFFECT MICROGRIPPER DESIGN FOR FORCE-REFLECTIVE TELEMANIPULATION OF A MICROSCOPIC ENVIRONMENT

Michael Goldfarb
Nikola Celanovic

Department of Mechanical Engineering
Vanderbilt University
Nashville, TN 37235

ABSTRACT

This paper describes the fundamental physical motivations for minimum surface effect design, and presents a microgripper that incorporates a piezoelectric ceramic actuator and a flexure-based structure and transmission. The microgripper serves effectively as a one degree-of-freedom prototype of minimum surface effect micromanipulator design. Data is presented that characterizes the microgripper performance under both pure position and pure force control, followed by a discussion of the attributes and limitations of flexure-based design. The microgripper is interfaced with a force-reflective macrogripper, and the pair controlled with a hybrid position/force scheme. Data is presented that illustrates the effective operation of the telerobotic pair.

1 INTRODUCTION

While many devices have been developed to increase the resolution of human vision, relatively little work has been done to increase the resolution of human dexterity. A force-reflective macro-master micro-slave telerobotic system could intelligently filter and scale mechanical information to enable dexterous manipulation of a microscopic environment. In this sense, movements could be scaled down in the forward path from the master to the slave, so that the slave duplicates the motion of the master on a much smaller scale. The forward path could additionally include intelligent filters to remove physiological tremor and any other unwanted artifacts of human motion, as well as unwanted gravitational effects, such as the weight of a tool. The backward path from the slave to the master could address deficiencies in human force sensitivity by magnifying the forces reflected from the microscopic environment to a level that is perceptible by the human operator. Coupled with a stereomicroscope, this technology can enable humans complete interaction with a microscopic environment.

1.1 Design for Control of Interaction

Since telemanipulation fundamentally entails mechanical interaction, a successful telemicrorobot will require some degree of force control. Effective implementation of such control is largely influenced by the open-loop behavior of the manipulator. In particular, the presence of hard nonlinearities such as backlash and Coulomb friction in a manipulator result in severe deterioration of position and especially force control. The study of direct-drive robots, for example, was borne out of the necessity to implement precision position and force control of robot manipulators for purposes of mechanical interaction. A direct-drive design significantly reduces the amount of backlash and Coulomb friction in the control plant. The elimination of these hard nonlinearities enables effective and accurate position, force, impedance, or admittance control of the robot manipulator.

Due to the physics of scaling, devices that operate on a microscopic scale are influenced by these nonlinear behaviors to a much greater degree than those of a conventional scale. Consequently, an effective micromanipulator that will enable dexterous manipulation in a microscopic environment cannot simply be fabricated as a scaled-down version of a macrorobot. Instead, development of a successful microrobot capable of accurate and competent force-controlled micromanipulation will necessitate elimination or intelligent minimization of surface force behavior.

1.2 Scaling

The types of forces that dominate mechanical dynamic behavior on a microscopic scale are different than those that dictate motion on a conventional scale. As an example, consider small insects which can stand on the surface of still water, supported only by the surface tension. The same surface tension is present when humans come into contact with water, but on a human scale the associated forces are typically insignificant. The world in which humans live is governed

by the same forces as that in which these small insects live, but the forces are present in very different proportions. For the purposes of mechanical dynamics, the forces that govern the motion of discrete objects can be classified as one of two types: body forces, which directly influence the entire volume of an object, and surface forces, which act primarily on the surface area of the object. In mechanical environments, the former are generally regarded as inertial forces, while the latter are classified as friction forces. The magnitudes of inertia and other types of body forces are typically proportional to the volume of an object, while magnitudes of friction and other types of surface forces are roughly proportional to the object's surface area. Since the ratio of surface area to volume of an object increases with decreasing size, the behavior of microscale devices is influenced principally by surface forces. The problem with this change in proportions is that interaction dominated by friction (surface) forces is far more difficult to control than that dominated by inertial (body) forces. Though inertial forces can become complicated by inertia-coupling, they are fundamentally smooth ($F=ma$, assuming $v \ll c$). Friction forces, especially those present during sliding, are typically highly nonlinear (i.e.: stick-slip phenomena). The net effect of surface-force-dominated behavior is at best severe deterioration of position and force control, and at worst complete instability. In addition to significantly impairing positioning performance, presence of large surface forces (with respect to control forces) renders endpoint forces either uncontrollable or unobservable, depending on the collocation or non-collocation of the actuator/sensor combination. Such behavior severely complicates the ability to measure and/or control endpoint forces, and thus makes detection and/or reflection of microscale forces an extremely difficult and ill-posed task, if possible at all.

1.3 Minimum Surface-Effect Design

Though a direct-drive configuration is sufficient to minimize the effects of hard nonlinearities in a macroscopic manipulator, the elimination of drive transmission alone will not sufficiently attenuate these behaviors on a microscopic scale. An effective force-controlled micromanipulator should therefore incorporate design techniques that will minimize highly nonlinear surface force behavior and thus enable effective control of micromanipulation. Just as direct-drive is essential to the design of an effective force-controlled macromanipulator, minimal surface-effect approaches are similarly essential to the effective design of a force-controlled micromanipulator.

1.4 Flexure-Based Design

One means of eliminating surface forces is by incorporating a flexure-based design. A flexure is one or a series of mechanical levers that are fabricated from a single piece of material. If properly designed, such a structure can approximate the motion of a complex kinematic linkage with negligible Coulomb friction and no backlash. Additionally, the absence of joints and bearing surfaces produces a clean device that is free of lubricants or other contaminants, and is thus extremely conducive to clean environments. One can imagine an entire multi-degree of freedom microrobot fabricated from a single piece of material. A single-piece design also lends itself quite well to recently-developed depositing and etching micromanufacturing techniques. The gripper design described in this paper is essentially a one degree-of-freedom investigation of a flexure-based microrobot design.

2 MICROGRIPPER DESIGN

2.1 Actuation

The human motor control system exhibits position and force bandwidths on the order of fifteen and five-hundred Hertz, respectively (Fischer et al., 1990). A transparent telemanipulation system therefore requires an actuator that exhibits comparable bandwidths and sufficient power to perform work in the environment of interest. Additionally, control stability is best served with open-loop stable actuators that are devoid of backlash and exhibit minimal surface force behavior. The range of motion and gripping force required of a microgripper are largely dependent upon application. The microgripper described in this paper was designed to offer a gripping workspace approximately two orders of magnitude smaller than the typical human prehensile grip. Such scaling requires a range of motion of 500 microns and suggests an appropriate gripping force of 500 mN.

Prior work by the authors indicate that piezoelectric ceramic, coupled with an intelligently-designed transmission (devoid of bearing surfaces), is a strong candidate for providing the desired actuation performance (Goldfarb and Celanovic, 1996). A typical lead-zirconate-titanate (PZT) piezoelectric actuator can perform step movements with a resolution on the order of a nanometer. These actuators offer open-loop stable operation with the power and bandwidth necessary for the specified motion. The primary inadequacy of the PZT as a microrobotic actuator is that the strain-based deformations that it provides are limited to approximately 0.1%. A piezoelectric stack that could provide the desired displacement of 500 microns in a direct-drive fashion would therefore have to be one half meter in length. Since piezoelectric ceramic actuators operate in compression, stack geometry is typically constrained by buckling considerations to significantly shorter lengths. The piezoelectric stack incorporated for actuation of the flexure-based microgripper, for example, is twenty millimeters in length (Tokin model #AE0505D16) and is therefore capable of approximately twenty microns of no load displacement. Incorporating a typical piezoelectric stack for actuation of the microgripper therefore requires a large ratio, frictionless amplification that is devoid of backlash.

2.2 Structure and Transmission

Minimum surface effect movement and power transmission is provided by a flexure-based linkage, as shown in Figure 1. The structure approximates the linkage illustrated in Figure 2, and provides a transmission ratio of about thirty to one and parallel closure of the gripping tongs. This transmission affords a total gripping motion and a maximum gripping force of approximately 500 microns and one Newton, respectively, from the PZT actuator. The gripper prototype is

36 mm long, 16.5 mm wide, and 5 mm thick. The gripper was fabricated from a single piece of 7075 aluminum alloy with a wire electrical discharge machine process.

2.3 Sensors

The flexure-based structure of the gripper was designed to decouple strains due to gripper position and force. This design enables the use of strain gages for independent measurement of gripper position and force, as shown in the data of Figure 5 and 7. The microgripper prototype, complete with sensors and PZT actuator (housed), is shown in Figure 3.

3 MICROGRIPPER PERFORMANCE

3.1 Position Control

A simple (digitally-implemented) proportional-integral-derivative (PID) controller was utilized for microgripper position control. The position control loop frequency response is shown in Figure 4. As indicated in the figure, the position control frequency response begins to roll off around 15 to 20 Hertz. This roll-off reflects limitations imposed by computational delays of the digitally-implemented controller. Closed-loop time domain behavior is illustrated by the tracking data shown in Figure 5.

3.2 Force Control

A simple proportional-integral-derivative (PID) controller was utilized for microgripper force control. The force control loop frequency response is shown in Figure 6. As the case with position control, the roll-off exhibited by the system reflects limitations imposed by computational delays of the digitally-implemented controller. Closed-loop time domain behavior is illustrated by the tracking data shown in Figure 7.

3.3 Teleoperative System Performance

Human interface with the microgripper is provided by a force-reflective macrogripper, which is shown in Figure 8. The device is actuated with a DC torque motor (PMI model #N12M4T), and incorporates a precision potentiometer (Midori model #CPP-35B) for position (and velocity) measurement and a strain gage based load cell for torque measurement. The macrogripper provides a range of motion of almost 10 cm and can exert a maximum continuous force of about 80 N. The teleoperative pair is controlled with a bilateral feedback system that incorporates a hybrid position/force controller for the microgripper and a modified force controller for the macrogripper. Microgripper control utilizes the macrogripper position signal as command, while the macrogripper control incorporates the microgripper force signal, superimposed upon a simulated spring and damper, as command. The simulated spring and damper provide a stable return force in a similar manner to a standard pair of forceps. Both position and force information is scaled for the appropriate state space. Figure 9 demonstrates system behavior for typical teleoperated gripping.

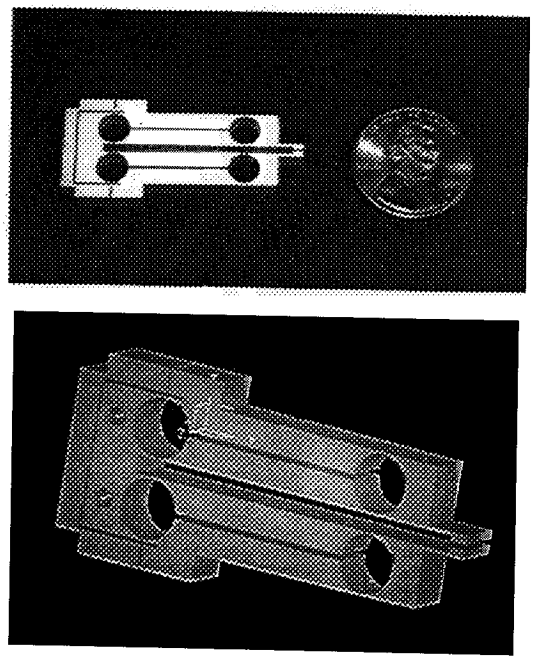

Figure 1. (TOP) Flexure-based microgripper structure and transmission and (BOTTOM) solid model of gripper design.

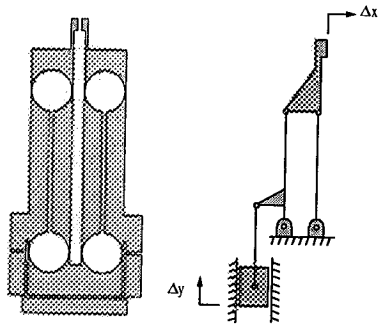

Figure 2. (LEFT) Two-dimensional drawing of microgripper structure and (RIGHT) idealized schematic of (one half of) flexure-based linkage.

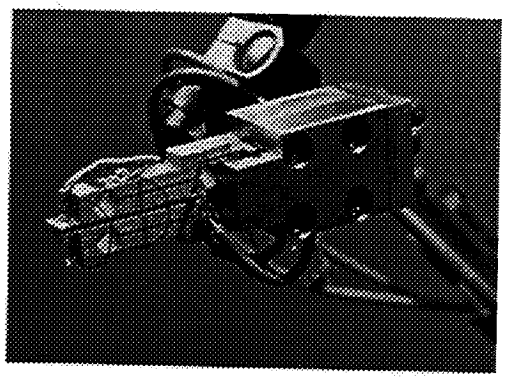

Figure 3. Instrumented microgripper prototype.

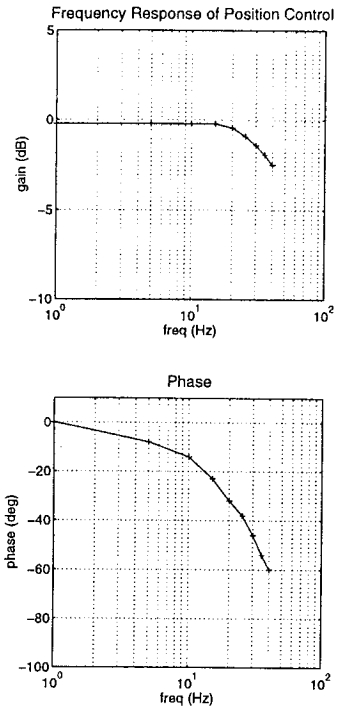

Figure 4. Frequency response of position control loop. Data was aquired at a 5 kHz controller sampling rate.

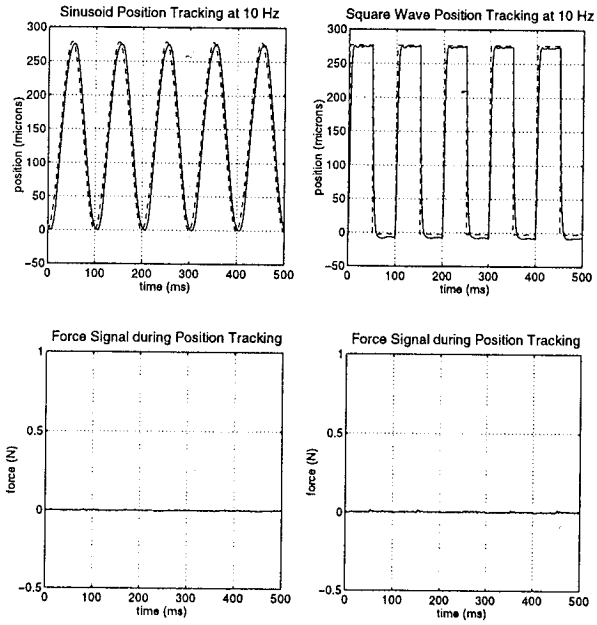

Figure 5. Closed-loop time domain behavior of position control loop for a 10 Hz sinusoid (LEFT COLUMN) and square wave (RIGHT COLUMN), showing the desired (dashed) and the actual (solid) position, and the corresponding force sensor signals (illustrating sensor decoupling).

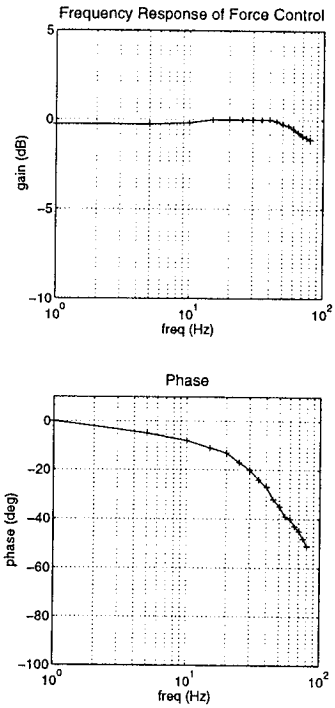

Figure 6. Frequency response of force control loop. Data was aquired at a 5 kHz controller sampling rate.

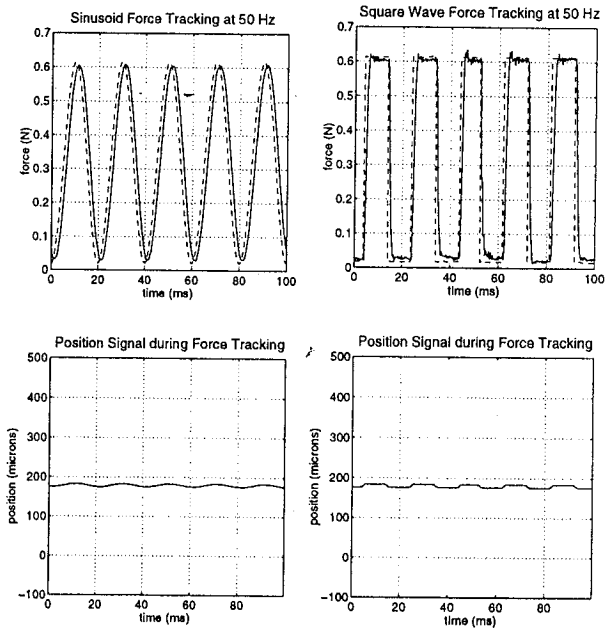

Figure 7. Closed-loop performance of force control for a 50 Hz sinusoid (LEFT COLUMN) and square wave (RIGHT COLUMN), showing the desired (dashed) and the actual (solid) force, and the corresponding position sensor signals. Note that the fluctuations in the position signal are due to object structural stiffness rather than fundamental sensor coupling.

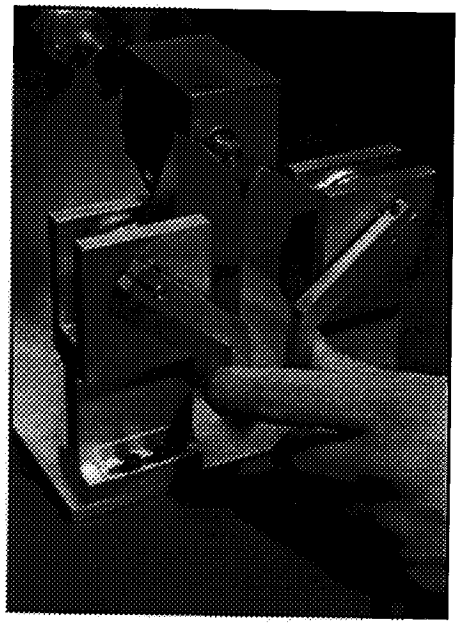

Figure 8. Force-reflective macrogripper for providing human interface with microgripper.

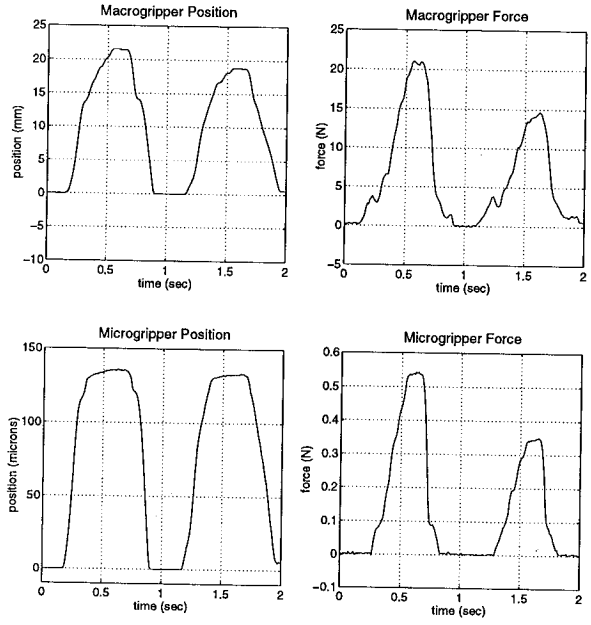

Figure 9. Typical data reflecting the behavior of the gripper pair during teleoperation. The data illustrates human-controlled gripping and releasing of a semi-rigid object.

4 DISCUSSION OF FLEXURE-BASED DESIGN

4.1 Flexure-Based versus Ideal Linkages

An ideal kinematic revolute joint is infinitely stiff in tension/compression and infinitely compliant in bending. A flexure-based joint has stiffness in bending and compliance in tension and compression. These differences in behavior impose several important limitations on flexure-based design. Perhaps the most significant is the limited angular motion of the flexure joints, which offer maximum angular displacements on the order of a few degrees. Greater range of motion could likely be achieved by utilizing plastic deformation, but such an approach would likely result in rapid fatigue failure. Some promising work has recently been conducted on the use of super-elastic flexure hinges that incorporate shape memory alloy and can achieve angular displacements up to thirty degrees (Horie et al., 1995). Super-elastic hinges, however, are geometrically more susceptible to tension/compression compliance and compressive buckling.

Another characteristic of a flexure-based linkage that is quite different from a kinematic chain is the inherent structural elasticity of the linkage. Since piezoelectric actuators are fundamentally unidirectional (they can provide only compressive force), this elastic behavior of flexure hinges can be advantageous, enabling bi-directional motion from a single PZT. This arrangement, however, renders one direction of motion a forced response and the other a characteristic response. Such a configuration entails a trade-off between a high positional bandwidth, which is dependent on a large joint stiffness, and a large output force, which is dependent on a low stiffness.

The combination of angular stiffness and compressive compliance of flexure joints presents another significant problem. Figure 10 shows an ideal kinematic mechanism for motion amplification and a flexure-based equivalent. The combined result of bending stiffness and compressive compliance in each joint is essentially lost motion. The addition of amplification stages in the ideal linkage would result in a greater output motion. The addition of stages in the flexure-based linkage, however, results in a stiffer structure and thus more compressive deformation of the hinges, the effects of which compound at some point to result in less output motion. The combination of bending stiffness and compressive compliance thus imposes practical limits on attainable flexure-based motion amplification.

4.2 Flexure Joint Geometry

A flexure-based linkage will most closely approximate an ideal linkage by minimizing the angular (bending) stiffness and maximizing the linear (compressive) stiffness. Rudimentary analysis of the flexure shown in Figure 11 gives some insight into design optimization. Assuming the flexure material is linearly elastic and defining the bending and compressive stiffnesses by the relations $M = k_b \Delta\theta_z$ and

$F = k_c \Delta x$, respectively, the stiffnesses of the flexure joint are given by:

$$k_b = \frac{EI}{L} = \frac{Ebh^3}{12L} \quad (1)$$

$$k_c = \frac{Ebh}{L} \quad (2)$$

where geometric variables are as defined in Figure 11, and E and I are the modulus of elasticity and area moment of inertia (about the z-axis), respectively. The ratio of bending to compressive stiffness is therefore:

$$\frac{k_b}{k_c} = \frac{h^2}{12} \quad (3)$$

where the units of this ratio are length squared per radian. This expression implies that optimal flexure behavior (as defined by this ratio approaching zero) is not affected by the material stiffness (E) and is best served by a thin flexure geometry ($h \rightarrow 0$). Analyses of flexure characteristics for more complex geometry's are given in (Paros and Weisbord, 1965) and (Ragulskis et al., 1989).

4.3 Scaling

A flexure-based design should be unaffected by surface-force behavior regardless of scale and should in fact exhibit increased structural bandwidth with decreasing scale. Utilizing etching, depositing, or lithography micromanufacturing techniques, for example, a similar device could be fabricated an order of magnitude smaller with likely improved dynamic performance. Position and force information can be measured with piezoresistive film (in place of strain gages) which can be deposited, along with electrical traces, directly on the surface of the flexure.

5 CONCLUSION AND FUTURE WORK

The flexure-based microgripper exhibits well-behaved, stable position and force control performance utilizing simple PID control. The minimum surface effect design approach would therefore seem quite well-suited for micromanipulator applications that entail mechanical interaction, such as a telemicrorobot. The minimum surface effect behavior of the flexure-based design, however, is bought at the cost of limited joint motion, joint stiffness in bending, and joint compliance in tension/compression. Present and future work involves continued investigation of minimal surface effect designs and the development of a multi-degree-of-freedom micromanipulator.

ACKNOWLEDGMENT

The work presented herein was supported by NASA Grant No. NAGW-4723. This support is gratefully acknowledged.

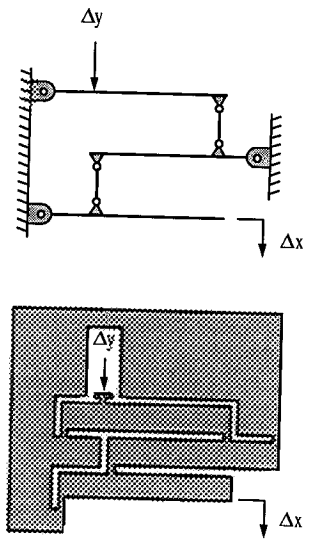

Figure 10. (TOP) Ideal kinematic mechanism for linear motion amplification and (BOTTOM) the flexure-based equivalent.

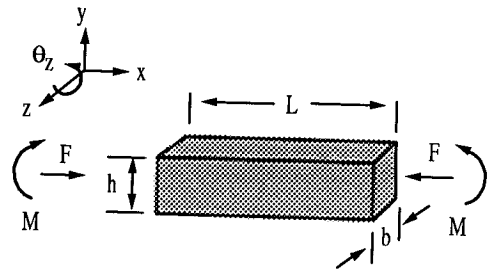

Figure 11. Geometrical definitions for a simplified flexure hinge.

REFERENCES

Fischer P., Daniel R., and Siva K.V., 1990, "Specification and Design of Input Devices for Teleoperation," Proceedings of the IEEE Conference on Robotics and Automation, pp. 540-545.

Goldfarb, M. and Celanovic, N., 1996, "Behavorial Implications of Piezoelectric Stack Actuators for Control of Micromanipulation," Proceedings of the IEEE Conference on Robotics and Automation, pp. 226-231.

Horie M., Nozaki T., Ikegami K., and Kobayashi, F., 1995, "Design System of Super Elastic Hingfes and its Application to Manipulator for Micro-Bonding by Adhesives," Proceedings of the International Symposium on Microsystems, Intelligent Materials, and Robots, pp. 185-188.

Paros, J. and Weisbord, L., 1965, "How to Design Flexure Hinges," Machine Design, Vol. 37, No. 27, pp. 151-156.

Ragulskis K., Arutunian M., Kochikian A., and Pogosian M., 1989, "A Study of Fillet Type Flexure Hinges and Their Optimal Design," Vibration Engineering, pp. 447-452.